AD-A118 432   WEATHER WING (7TH) SCOTT AFB IL   F/G 20/14
RAY-TRACING ANALYSIS OF A LINE-OF-SIGHT COMMUNICATIONS PATH.(U)
MAY 82 J W GOLDEY

UNCLASSIFIED 7WW/TN-82/001   SBI-AD-E850 179   NL

1 OF 1

END
DATE
FILMED
09-82
DTIC

TECHNICAL NOTE

7WW/TN-82/001

RAY-TRACING ANALYSIS OF A LINE-OF-SIGHT COMMUNICATONS PATH

BY

JAMES W. GOLDEY, MAJOR, USAF

MAY 1982

APPROVED FOR PUBLIC RELEASE; DISTRIBUTION UNLIMITED

7TH WEATHER WING (MAC)

SCOTT AFB, ILLINOIS 62225

REVIEW AND APPROVAL STATEMENT

The 7WW/TN-82/001, RAY-TRACING ANALYSIS OF A LINE-OF-SIGHT COMMUNICATIONS PATH, April 1982, is approved for public release. There is no objection to unlimited distribution of this document to the public at large, or by the Defense Technical Information Center (DTIC) to the National Technical Information Service (NTIS).

This report has been reviewed and is approved for publication.

Steven L Erickson

STEVEN L. ERICKSON, Maj, USAF
Chief, Staff Support Liaison Division
Reviewing Officer

FOR THE COMMANDER

Richard A Rasmussen

RICHARD A. RASMUSSEN, Maj, USAF
Chief, Aerospace Sciences Division

29 APR 1982

REPORT DOCUMENTATION PAGE

READ INSTRUCTIONS BEFORE COMPLETING FORM

1. REPORT NUMBER
7WW/TN-82/001

2. GOVT ACCESSION NO.
AD-A118 432

3. RECIPIENT'S CATALOG NUMBER

4. TITLE (and Subtitle)
RAY-TRACING ANALYSIS OF A LINE-OF-SIGHT COMMUNICATIONS PATH

5. TYPE OF REPORT & PERIOD COVERED
Technical Note

6. PERFORMING ORG. REPORT NUMBER

7. AUTHOR(s)
James W. Goldey, Major, USAF

8. CONTRACT OR GRANT NUMBER(s)

9. PERFORMING ORGANIZATION NAME AND ADDRESS
7th Weather Wing
Staff Support Liaison Division
Scott AFB, Illinois 62225

10. PROGRAM ELEMENT, PROJECT, TASK AREA & WORK UNIT NUMBERS

11. CONTROLLING OFFICE NAME AND ADDRESS
7th Weather Wing
Staff Support Liaison Division
Scott AFB, Illinois 62225

12. REPORT DATE
May 1982

13. NUMBER OF PAGES
28

14. MONITORING AGENCY NAME & ADDRESS (if different from Controlling Office)

15. SECURITY CLASS. (of this report)
Unclassified

15a. DECLASSIFICATION/DOWNGRADING SCHEDULE

16. DISTRIBUTION STATEMENT (of this Report)
Approved for public release; distribution unlimited.

17. DISTRIBUTION STATEMENT (of the abstract entered in Block 20, if different from Report)

18. SUPPLEMENTARY NOTES

19. KEY WORDS (Continue on reverse side if necessary and identify by block number)
Meteorology
Ray Tracing
Atmospheric Refraction
Radio Holes
Telecommunications
Adenau, West Germany
Feldberg, West Germany

20. ABSTRACT (Continue on reverse side if necessary and identify by block number)
This report describes a ray-tracing technique used to examine possible causes of a line-of-sight microwave link between Feldberg and Adenau, West Germany during the winters of 1975-76 and 1976-77. Use of the technique with various model atmospheres helped determine the significance of refractive bending and the location of radio holes. Estimates of the depth of the resulting fades showed that, on the average, fade was not significant. Results showed that fade can be expected whenever surface-based trapping layers extend to 1800 feet MSL. Antenna decoupling, another possible source, was not examined in this study.

PREFACE

This report examines the performance of a line-of-sight microwave link with a ray-tracing technique that simulates the propagation of the microwave radiation through various model atmospheres. The ray-tracing technique is used to determine the significance of induced refractive bending. This information should be useful to radio engineers as well as radio meteorologists, especially those examining the climatology of "significant" weather events. The locations of radio holes under various propagation conditions and an estimate of the depth of resulting fades are presented.

CONTENTS

ILLUSTRATIONS

TABLES

RAY-TRACING ANALYSIS OF A LINE-OF-SIGHT COMMUNICATIONS PATH

Introduction

This report presents the results of a study to determine causes of a high incidence of reported propagation outages on several Defense Communications Systems (DCS) wideband line-of-sight (LOS) links in central Germany during the period October 1975 to February 1976 and again during the winter of 1976-1977. Although there was strong evidence for the presence of temperature inversions in the region, no specific data on height or intensity of the inversion layers could be obtained along a particular LOS path. Thus, there was no direct evidence as to what specific condition(s) of the atmosphere caused the outages. It therefore becomes impossible to predict whether any techniques could be employed to overcome the problem. Additionally, climatologists cannot easily predict the frequency of "significant" weather events (as they affect path performance) in the future.

This study uses a modeled atmosphere and assumes horizontal homogeneity of the refractive profile and a flat surface between transmit and receive antennas. Ray-tracing analysis helps infer the location and vertical extent of radio holes relative to the height of the receive antenna. By this process one can define which atmospheric refractivity conditions may be significant enough to degrade path performance through the modeled atmosphere. This study does not address multipath fading, antenna decoupling, or other types of atmospheric-induced signal loss.

Transmissions in one direction only for the path from Feldberg to Adenau (crossing the Rhine River) are examined. The path from Feldberg to Adenau is 103 km (55.9 NM) long. The Feldberg site transmits at 8 GHz from a 10-foot antenna, with a centerline takeoff angle at Feldberg of -0.39 degrees and 0.85-degree beamwidth. The predicted received signal level (RSL) is -31.7 dBm and the fade margin is 47.2 dB. The height of the transmitter at Feldberg is 2473 feet mean sea level (MSL), and the height of the receiver at Adenau is 2223 feet MSL. Significant potential path obstructions (mountain peaks) were obtained from the path profile. These are drawn on Figure 1 and are represented on the ray-tracing plots.

Modeling Technique

Although evidence pointed to the presence of temperature inversions during propagation outages in the winter of 1975-1976, no quantitative evaluation was performed to determine the strength of the inversion along the LOS path. Neither were there reliable representative data on the moisture lapse through the suspected layers. Both temperature and moisture, as well as pressure data, are required to compute atmospheric refractivity through the vertical extent of the atmosphere. Since the bending of electromagnetic energy propagating through the atmosphere is determined by the vertical gradient of refractivity, that gradient must either be measured or modeled.

In this study 12 different profiles of atmospheric refractivity were constructed. In 11 cases (Figure 1, profiles 2 through 12) a surface-based trapping layer (-50N/1000 feet) was assumed with the top of the layer varying from 1200 feet to 2500 feet MSL. The profiles were assumed standard (-12N/1000 feet) above the layers. In the last case (Figure 19), the gradient of the surface-based layer was increased to -100N/1000 feet. The top of the layer was at 2500 feet and standard conditions were assumed above that level.

The computer program used to generate "rays" of energy from the transmitter could present 20 rays at one time. The first effort in the ray-tracing analysis was to generate sufficient rays to encompass the entire beamwidth with a ray incrementation of 0.05 degrees. As the general location of resulting "holes" was established, the range of angles was selected so as to define the hole more precisely and a bundle of 20 rays with 0.01-degree incrementation was generated.

Ray-Tracing Analysis

As can be seen from the ray-tracing plots, trapping layers that extend from the surface to 1200-, 1400-, and 1600-feet MSL (Figures 2 through 4) create holes at the range corresponding to the path length; however, these holes appear below the height of the receiver. (In all cases the rays reflected from the horizontal axis of the graph are to be ignored.) Figure 5 depicts a layer extending up to 1800 feet MSL; a resulting hole just reaches the receiver. A closer look at the hole is presented in Figure 6. With layer tops from 1900 feet to 2400 feet (Figures 7-16), the receiver is within the hole. As the top of the surface-based layer reaches 2500 feet, the beam again falls on the receiver (Figure 17). However, since the entire beam as displayed is within the trapping layer, it is bent downward considerably. Recalling that the centerline takeoff angle is -0.39 degrees and the beamwidth 0.85 degrees, the half-beamwidth of the half power point (-3 dB) is at +0.035 degrees on the upper portion of the beam. Thus, the intercepted or received signal in Figure 17 should be stronger than -3 dB. In addition, there is still a hole present. Although not shown in this figure, it is located above the receiver and is even larger than in previous cases. (Remember, in each of these cases we are dealing with a modeled atmosphere. Actual radio holes at the receive antenna would depend on many factors, e.g., atmospheric refractivity, surface obstructions (mountains) along the path, etc.)

Figure 18 is a composite presentation of the vertical extent of the "model" holes relative to the height of the receive antenna for profiles 5-11. From this presentation, it appears that there is an irregular increase in the height of the bottom of the hole, while the top of the hole increases nearly linearly, at least through profiles 5-9. It must be pointed out that the hole presented represents the vertical distance between two successive rays separated by 0.01 degrees as they emanate from the antenna. Another choice of ray incrementation ,e.g., 0.001 degrees, would define the hole somewhat differently, but generally should diminish only the vertical extent of the hole. The approach generally taken to determine the significance of a hole is to examine the spreading or divergence of rays in the hole relative to the spreading elsewhere (above or below the hole). One may then infer qualitatively the strength of the hole. While the choice of ray incrementation will alter the absolute size of the hole, the spacing relative to the divergence of other rays will remain the same. Thus, a subjective determination of the strength of a hole is independent of ray incrementation.

This concept of ray spacing led to the postulation of an objective method to determine the fading in a radio hole. This technique employes principles of energy conservation and assumes that the average power density between any two rays in the bundle being examined is the same when leaving the transmitter. The assumption is not strictly true since through a half-beamwidth the signal decreases by 3 dB. However, it is a good approximation when examining rays within the half-beamwidth. The equation for the amount of fading in dB is

$$F(\mathrm{dB}) = 10 \log \Delta H/\Delta H' \qquad (1)$$

where ΔH is the vertical spacing between successive rays in the unaffected portion of the beam, and $\Delta H'$ is the spacing in the hole. The fading computed by Equation (1) does not specify the distribution of power across the hole--only the average fade within the increment.

The output from the ray-tracing program provided the height of each ray at specified ranges. Using the values of ray heights at the range of the receiver for each profile, the average ray spacing below the hole and the vertical extent of the hole were computed to assign values to ΔH and $\Delta H'$, respectively. Using these in Equation (1) gives the average fade within the hole, Table 1.

Table 1. Average Fade (F) Within the Hole.

Profile #	5	6	7	8	9	10	11
F (dB)	-7.7	-6.6	-8.4	-8.7	-10.2	-9.9	-11.6

The values for fading in the holes presented in the table do not appear significant. However, those values are meant to represent the average fade within the ray increment. There is no direct way to determine the absolute minimum signal in the fade region. Also, the above values will be minimized because the rays below the hole are affected by the refractivity gradient through the layer. They will be bent downward more in the trapping layer than under standard propagation conditions. In addition, the vertical spacing between successive rays will be greater than under normal conditions. However, even if ray spacing in this portion of the beam were halved, the depth of the fade would increase by only 3 dB.

Conclusion

Fading on the LOS link from Feldberg to Adenau can be expected whenever surface-based trapping layers extend to 1800 feet MSL. This fading would be due to a radio hole in the vicinity of the receiver. The upper limit on the trapping layer height that would have a significant affect on the received signal is directly related to the strength of the layer. A trapping layer with a gradient of -50N/1000 feet extending to 2500 feet MSL will create a hole above the receiver (Figure 17). However, increasing the gradient to -100N/1000 feet in the same layer places the receiver in the middle of the hole (Figure 19).

Reorientation of the antennas (changing the angle) would not alter the affects of the hole. Similarly, changing the size of the receive antenna (inversely related to beamwidth) would not gain an advantage if there is no energy available due to the hole. If the range of layer heights examined were realistic, even changing the height of the antennas would not improve the path reliability. However, if climatologists determine that layers above a certain height have a significantly low probability of occurrence, then a choice of solutions will be more obvious.

Another source of fading that is possible on an LOS link is antenna decoupling due to the received energy (rays) falling outside the main lobe of the receiver. None of the cases examined led to such conditions. The propagation conditions necessary for this type of fade would be extremely strong refractivity gradients (about -200N/1000 feet) extending through much higher layers.

An additional observation from this study is that any meteorological testing of this path will necessarily entail measurements somewhere along the path. A test had tentatively been proposed to instrument each end of the path by placing meteorological sensors on the tower at multiple levels. However, detection of layers extending up to 1800 to 2100 feet would not be possible with such instrumentation due to the tower's topographic siting. Radiosondes, acoustic sounders, or tethered balloons would have to be used to define significant trapping layers intercepting the beam over its midpath.

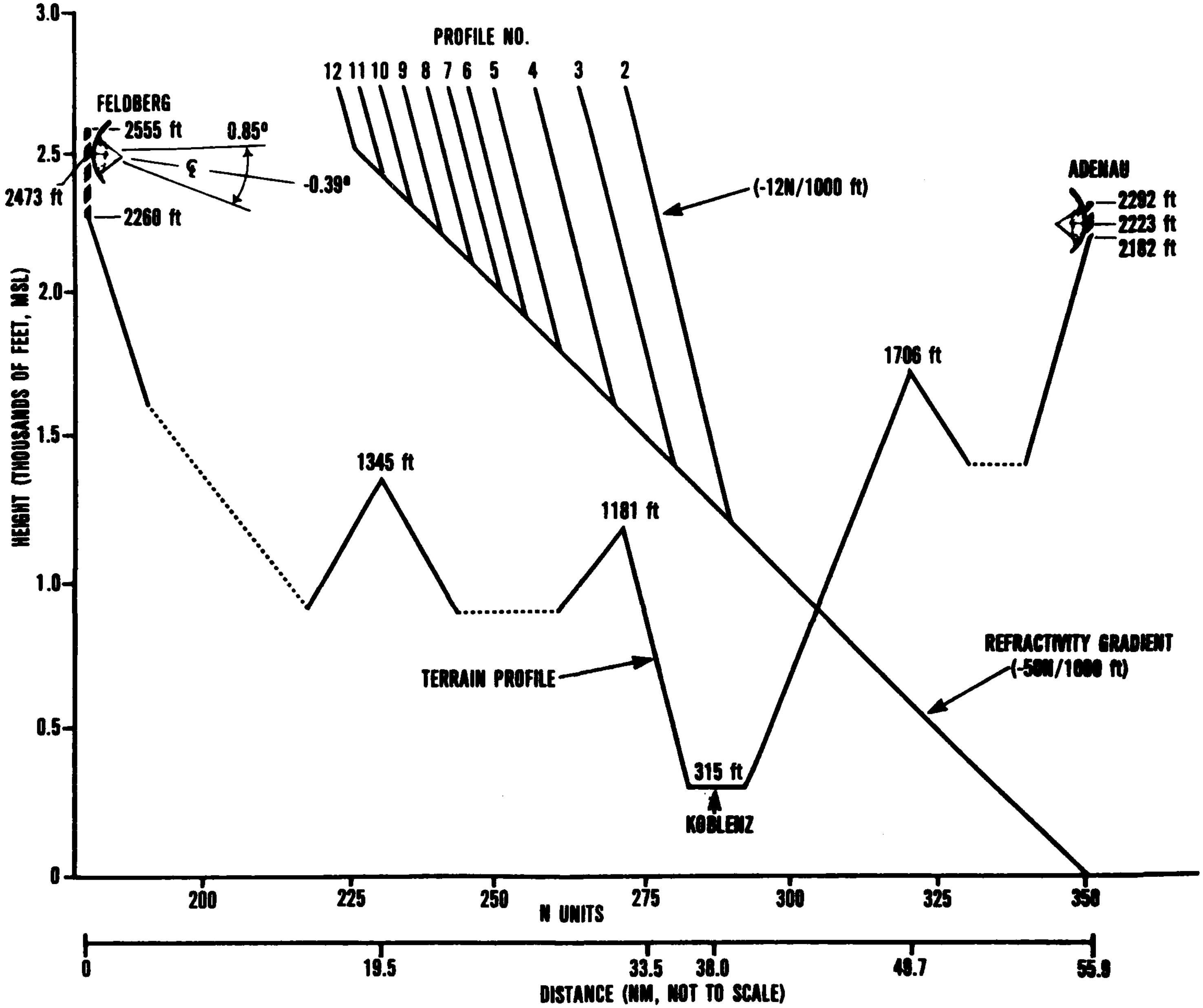

Figure 1. Path Profile and Model Refractivity Gradients

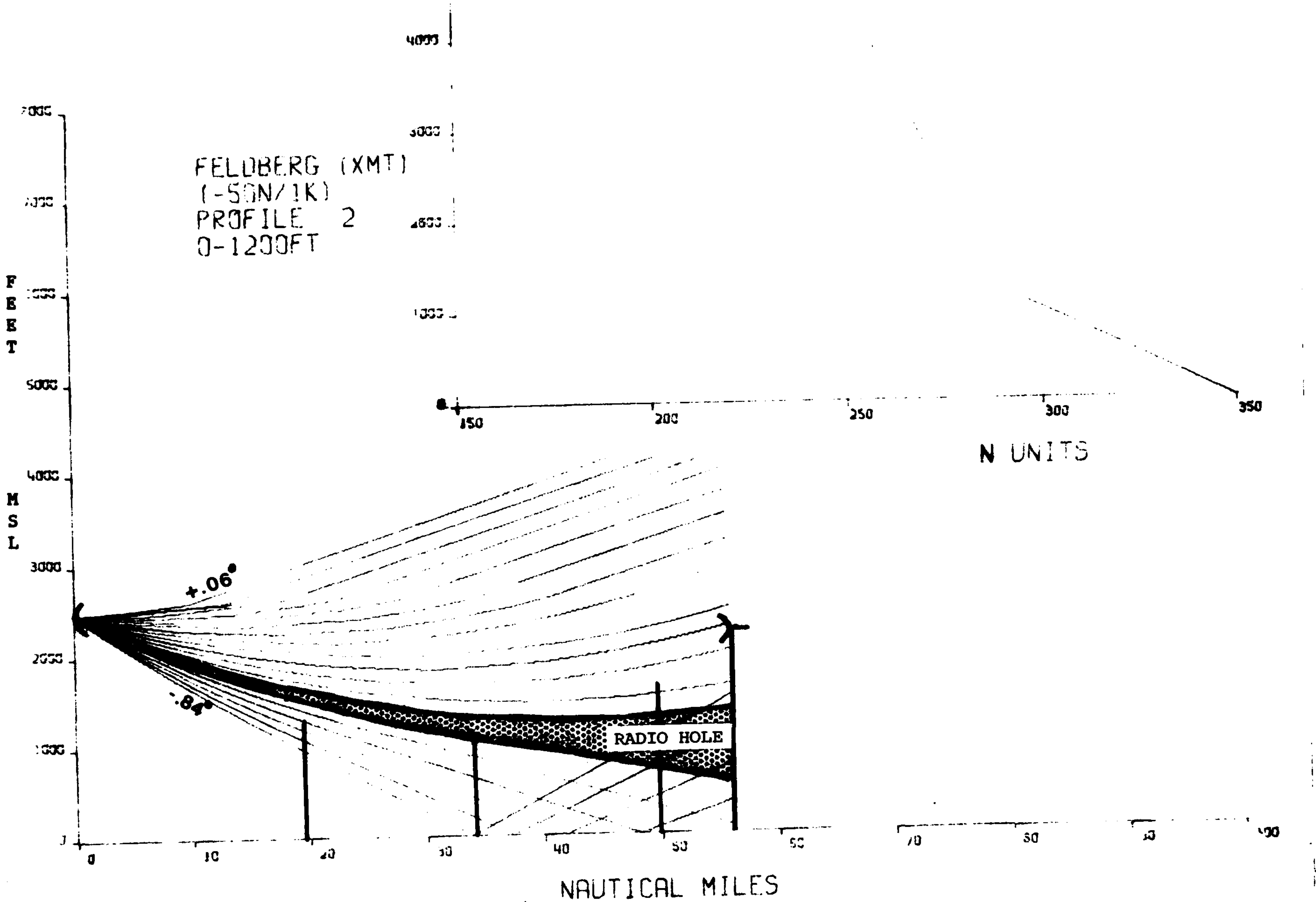

Figure 2. Refractivity Profile #2 and Ray Tracing for Layer 0-1200 ft MSL

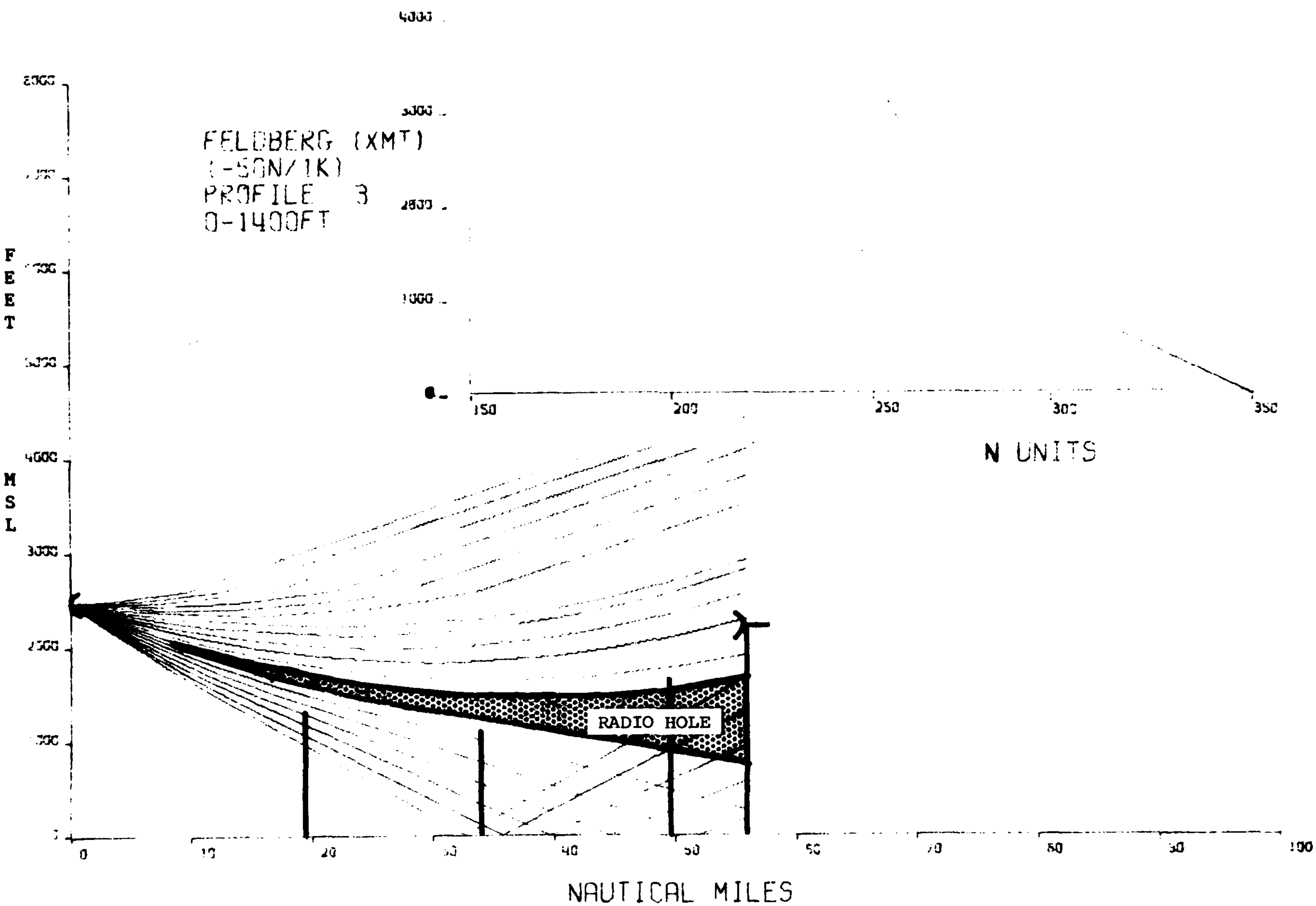

Figure 3. Refractivity Profile #3 and Ray Tracing for Layer 0-1400 ft MSL

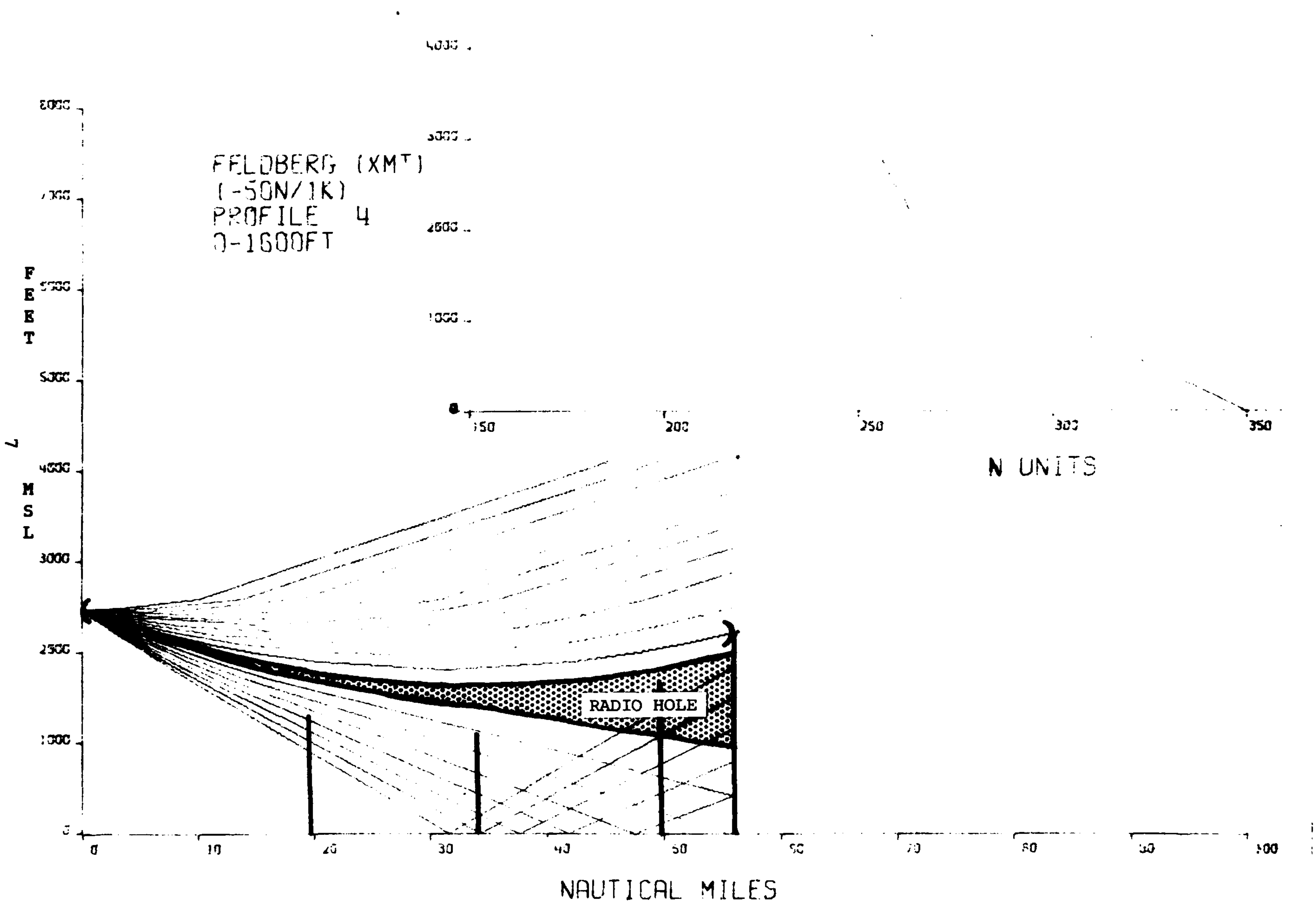

Figure 4. Refractivity Profile #4 and Ray Tracing for Layer 0-1600 ft MSL

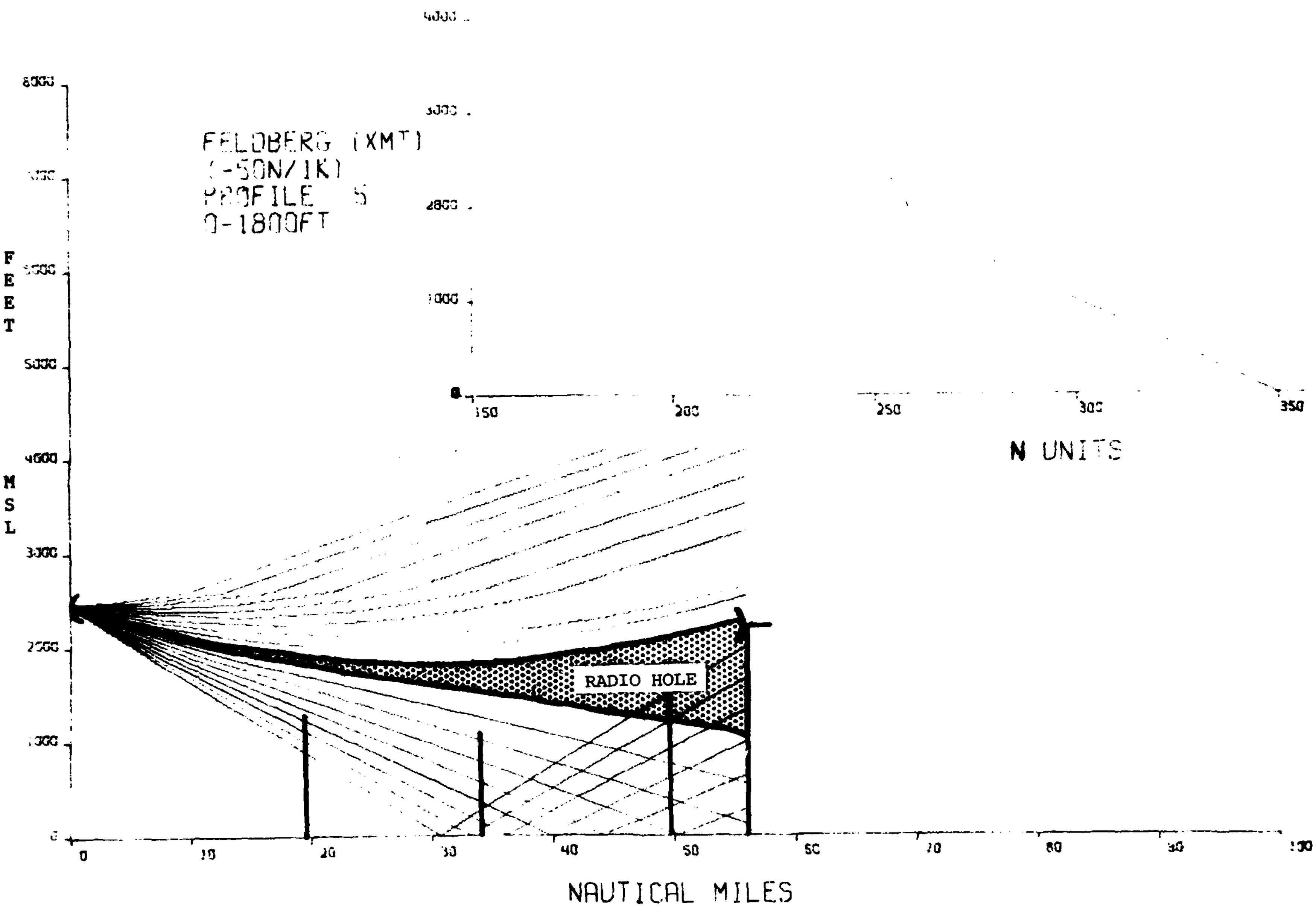

Figure 5. Refractivity Profile #5 and Ray Tracing for Layer 0-1800 ft MSL

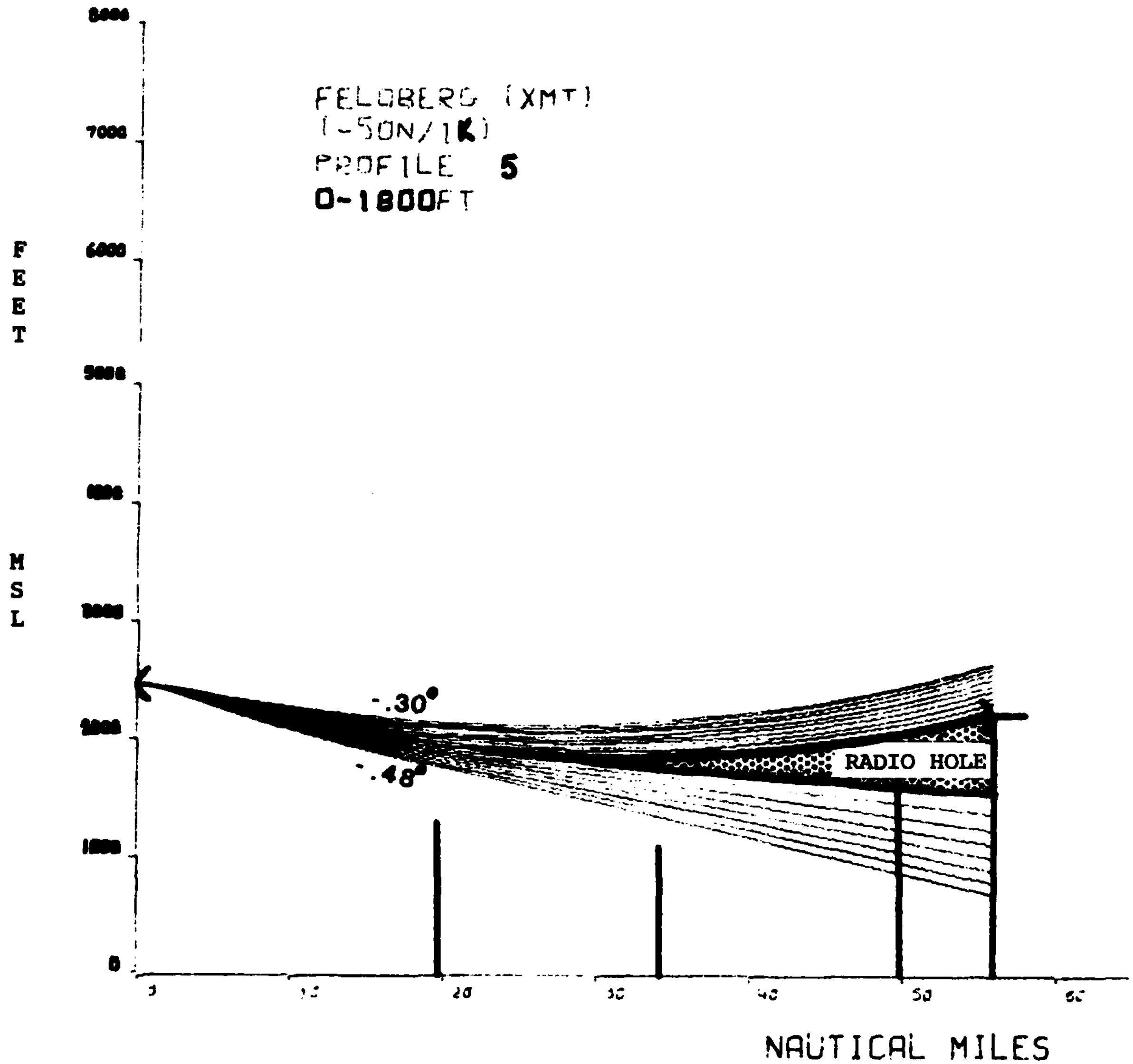

Figure 6. Detail of Ray Tracing for Profile #5

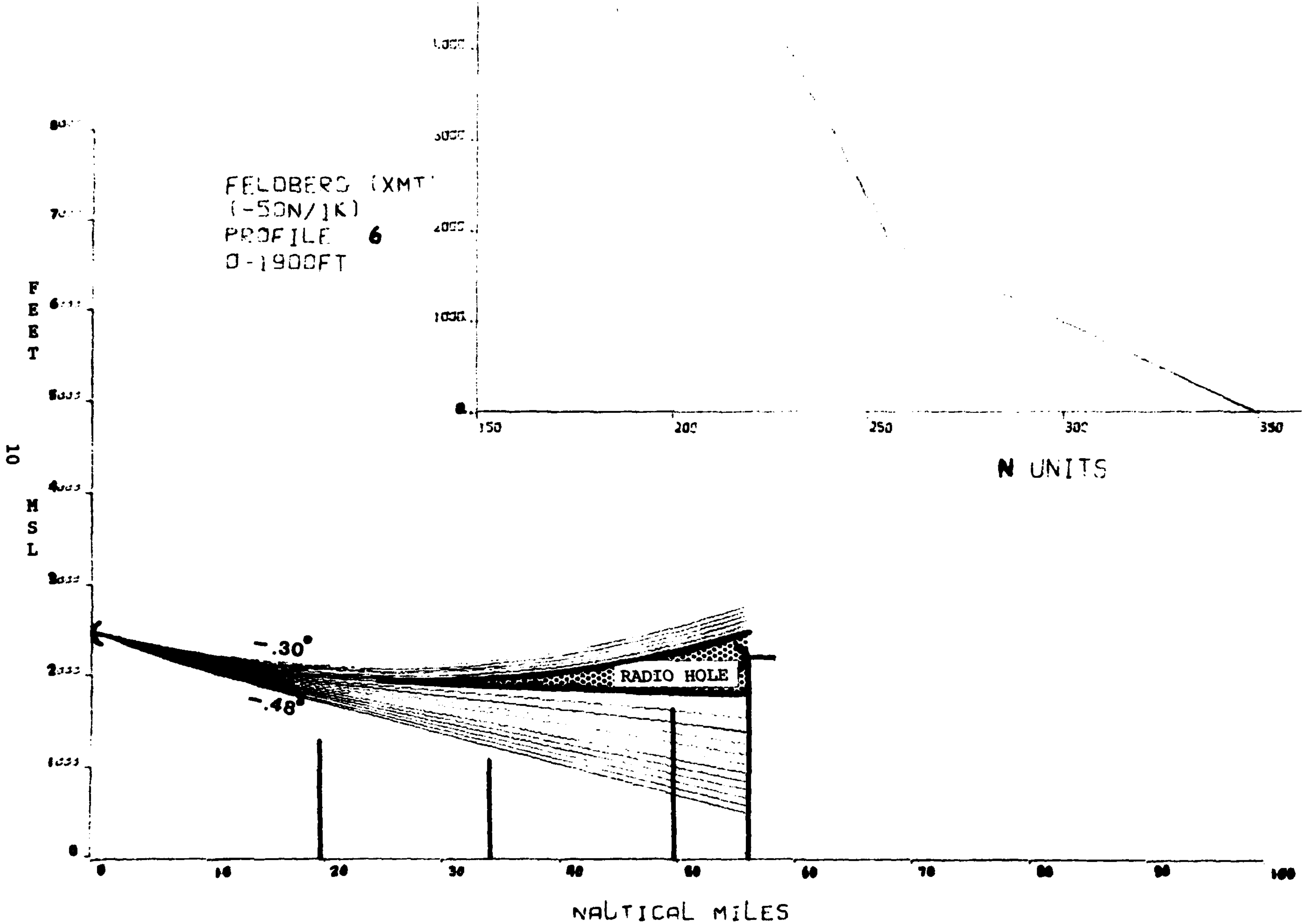

Figure 7. Refractivity Profile #6 and Ray Tracing for Layer 0-1900 ft MSL

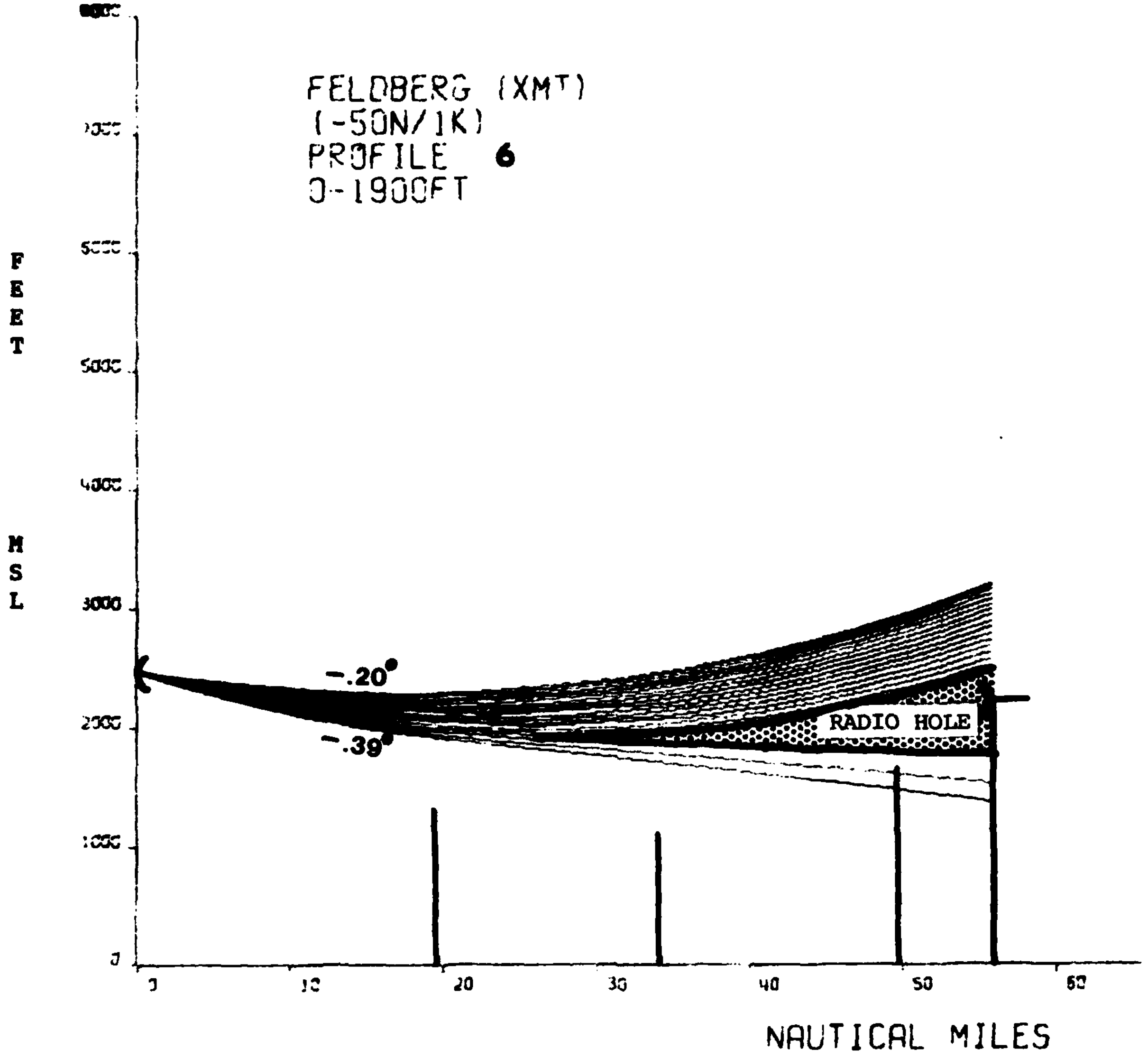

Figure 8. Detail of Ray Tracing for Profile #6

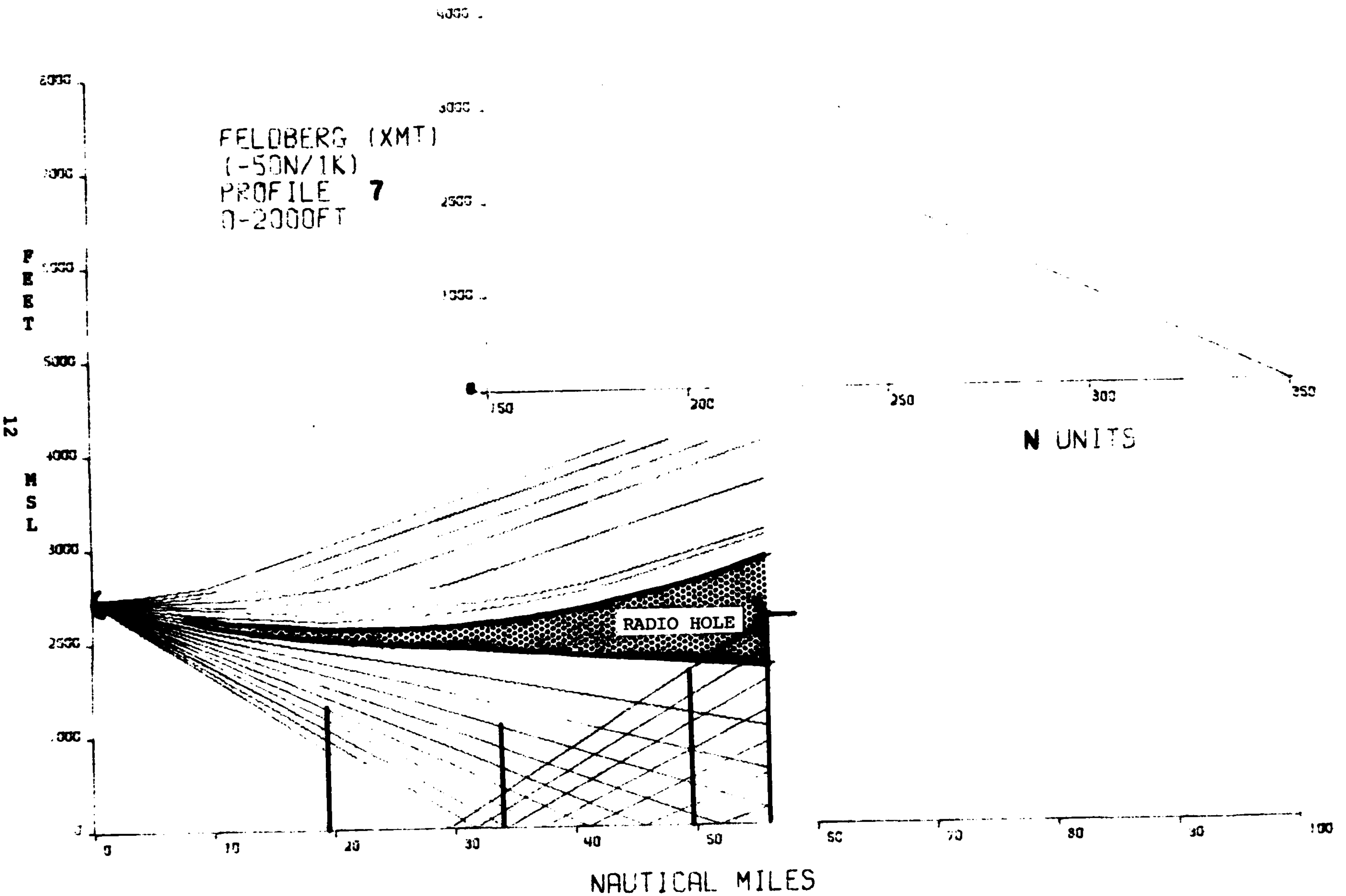

Figure 9. Refractivity Profile #7 and Ray Tracing for Layer 0-2000 ft MSL

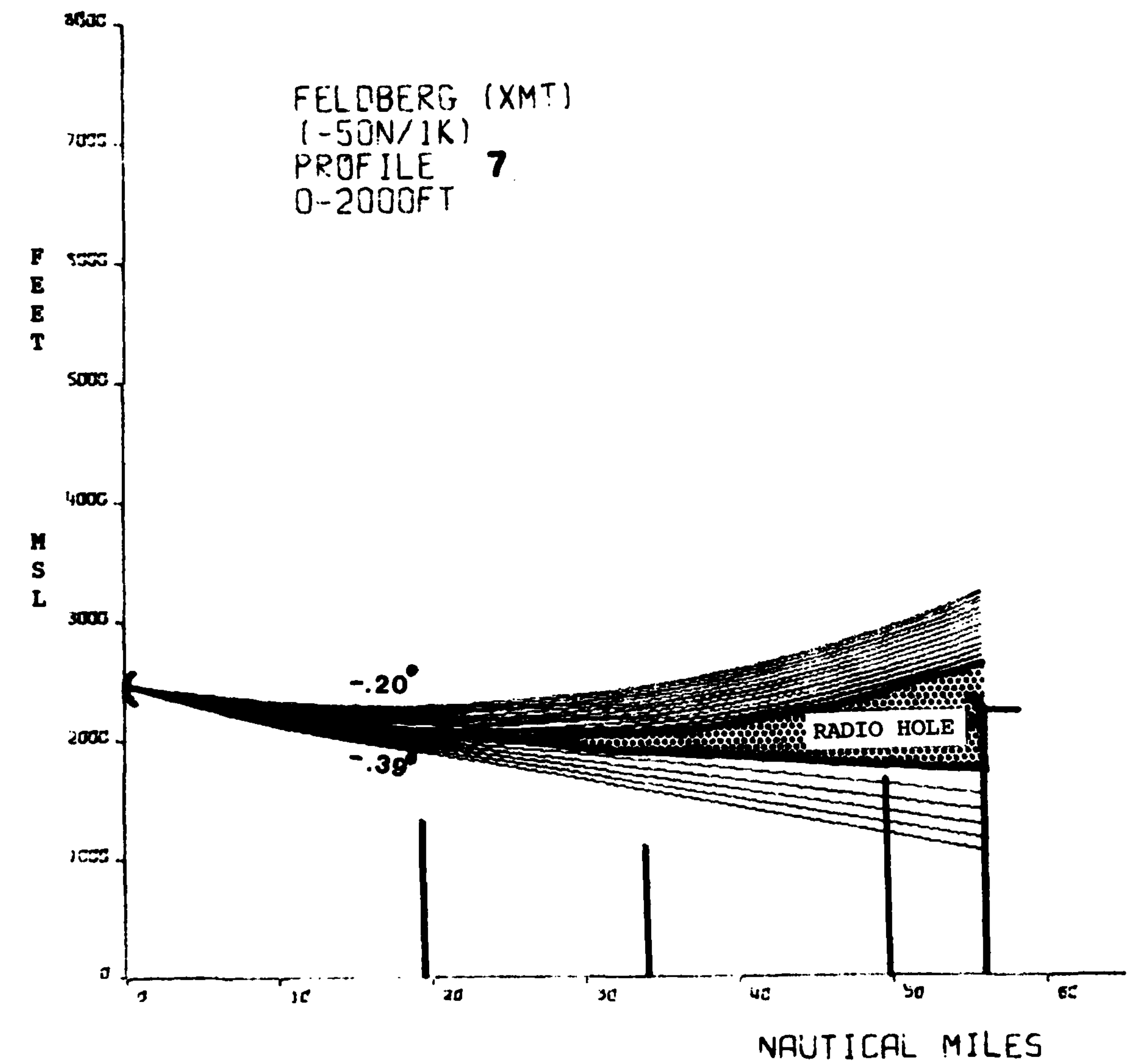

Figure 10. Detail of Ray Tracing for Profile #7

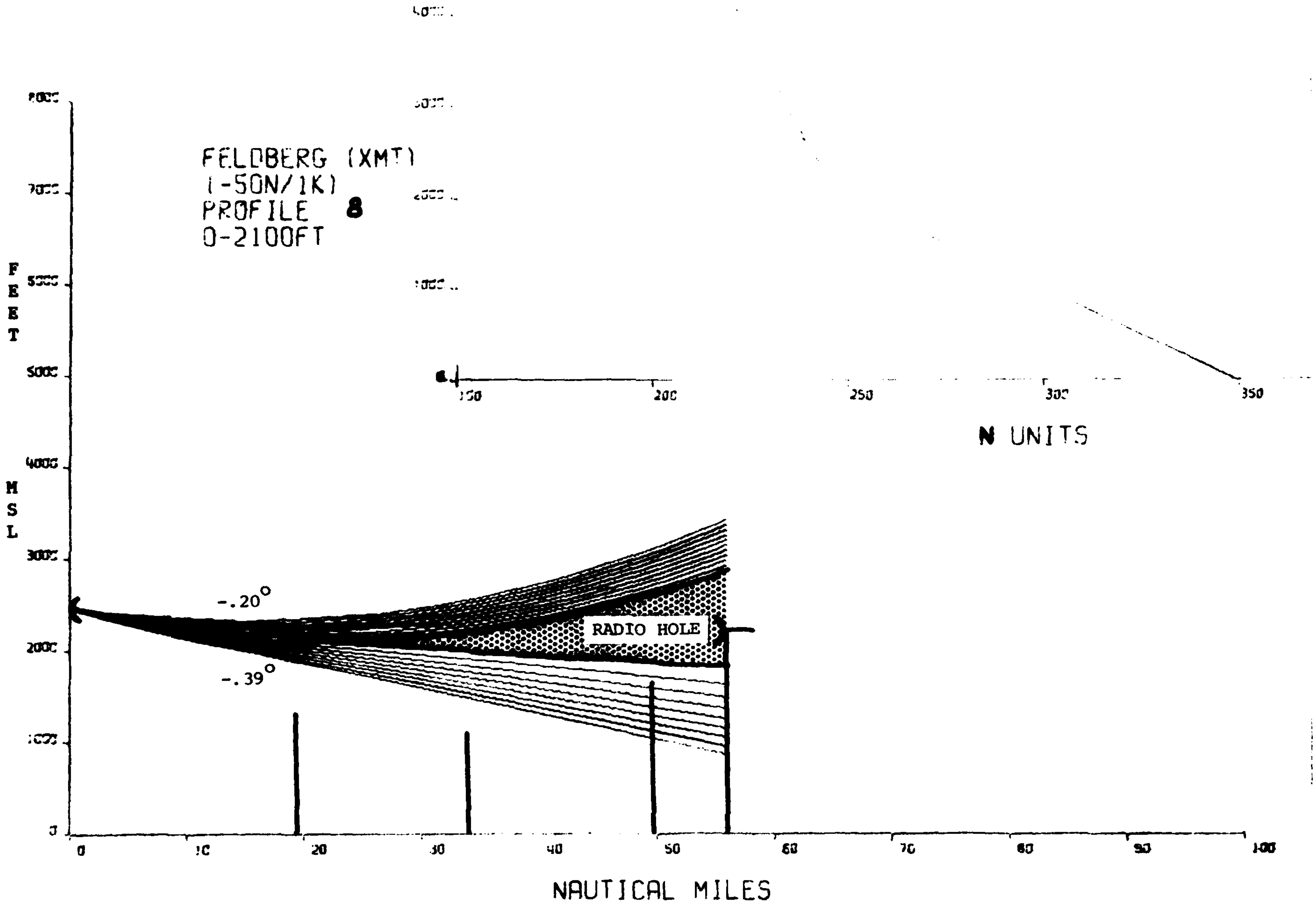

Figure 11. Refractivity Profile #8 and Ray Tracing for Layer 0-2100 ft MSL

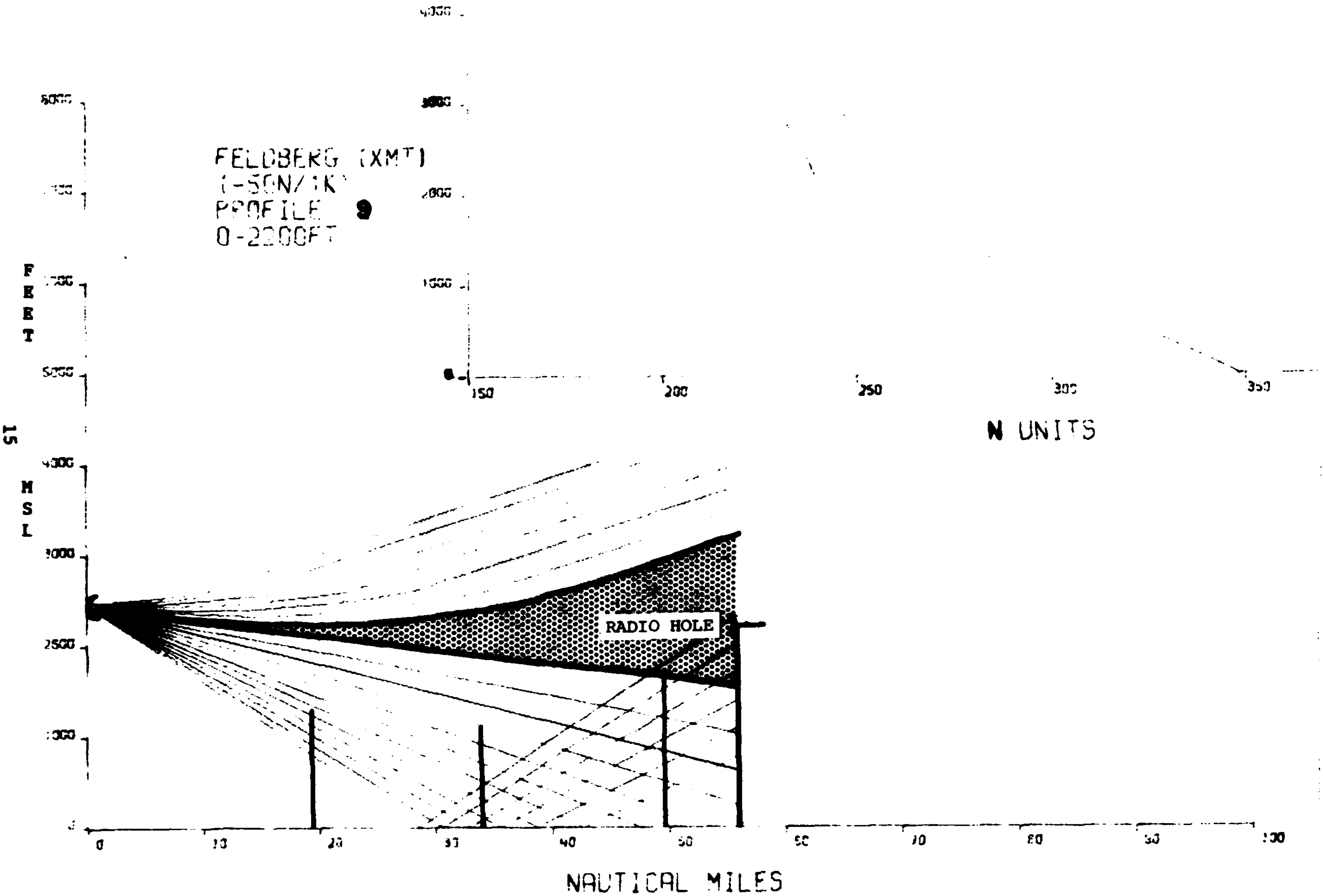

Figure 12. Refractivity Profile #9 and Ray Tracing for Layer 0-2200 ft MSL

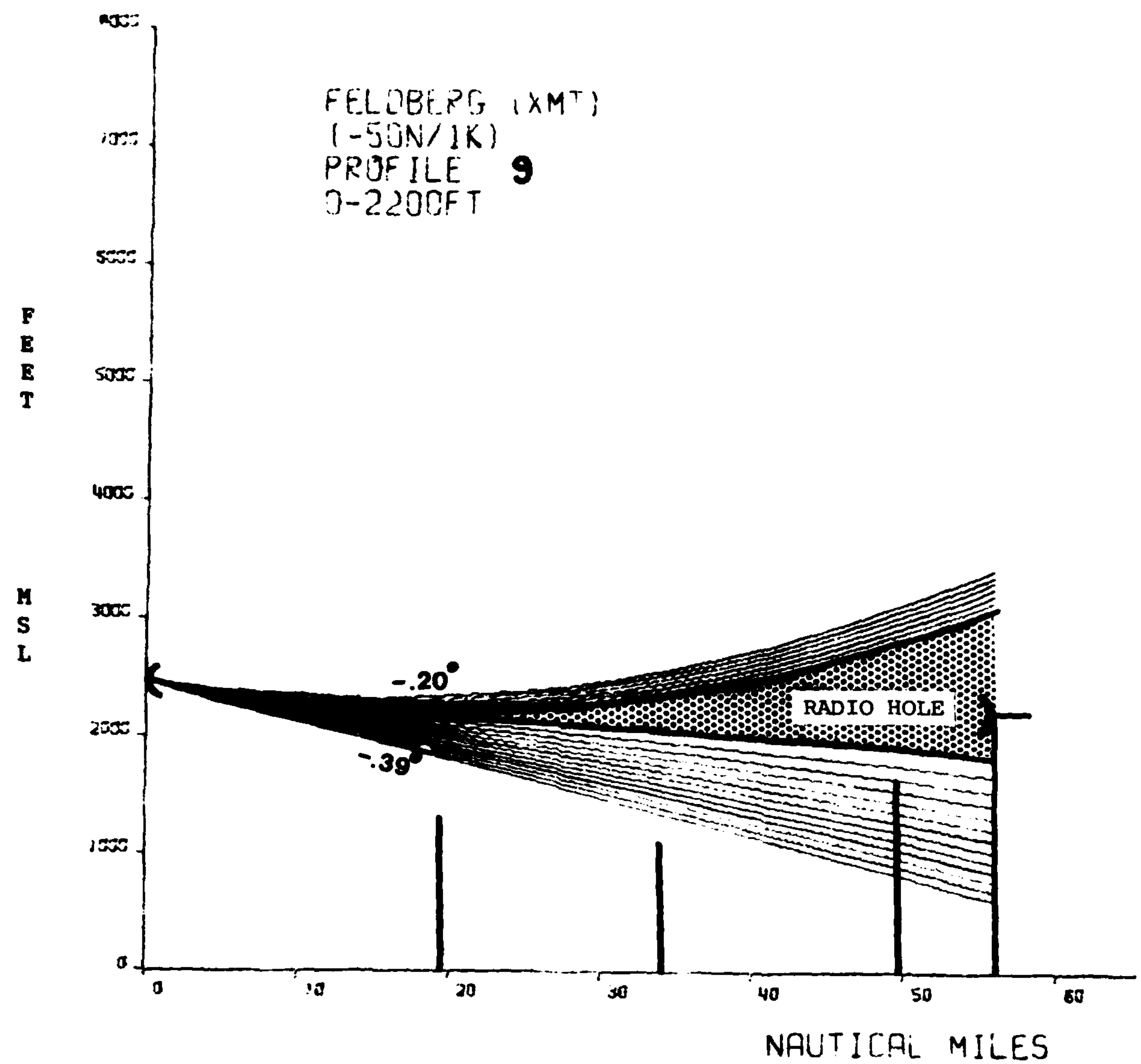

Figure 13. Detail of Ray Tracing for Profile #9

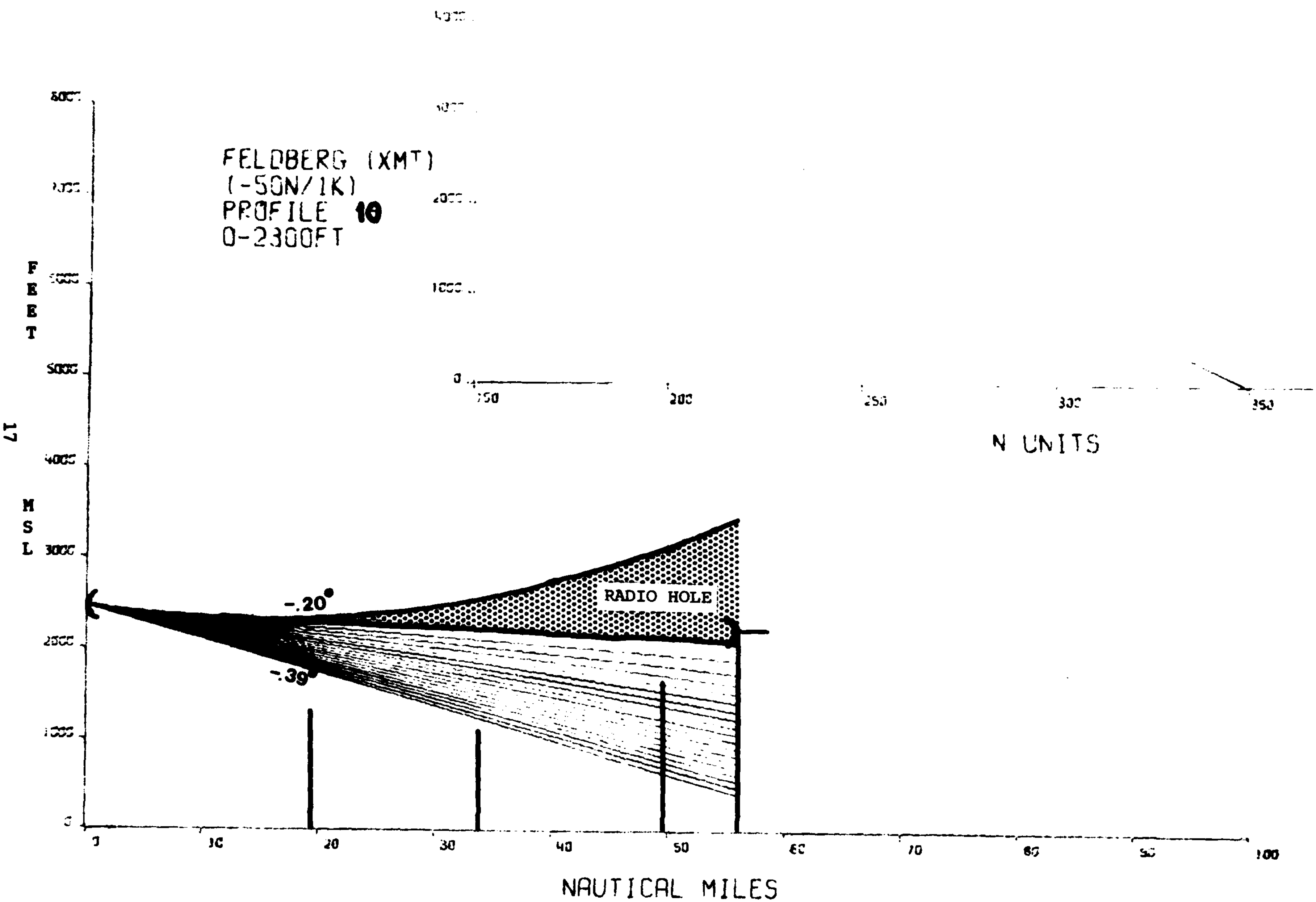

Figure 14. Refractivity Profile #10 and Ray Tracing for Layer 0-2300 ft MSL

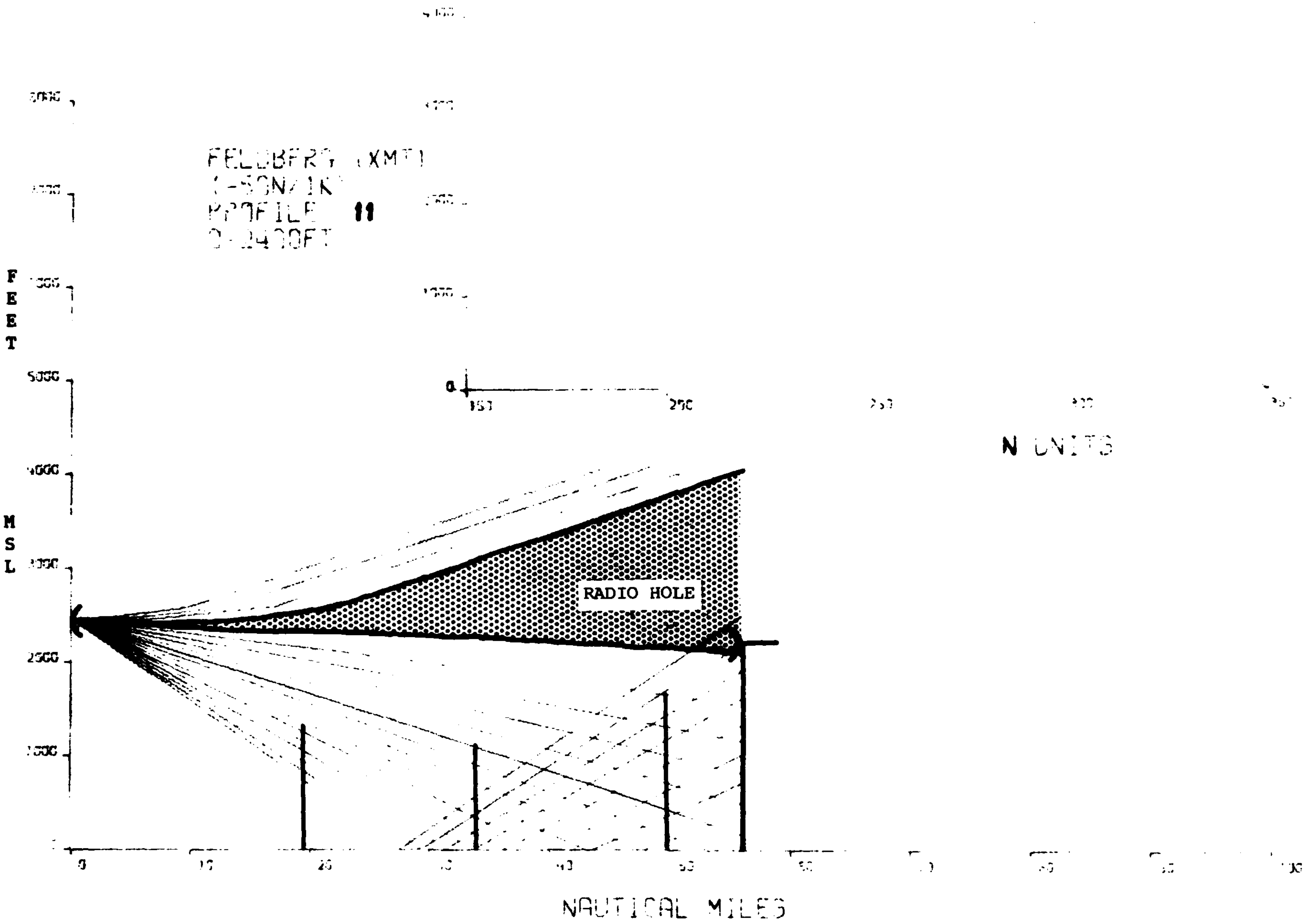

Figure 15. Refractivity Profile #11 and Ray Tracing for Layer 0-2400 ft MSL

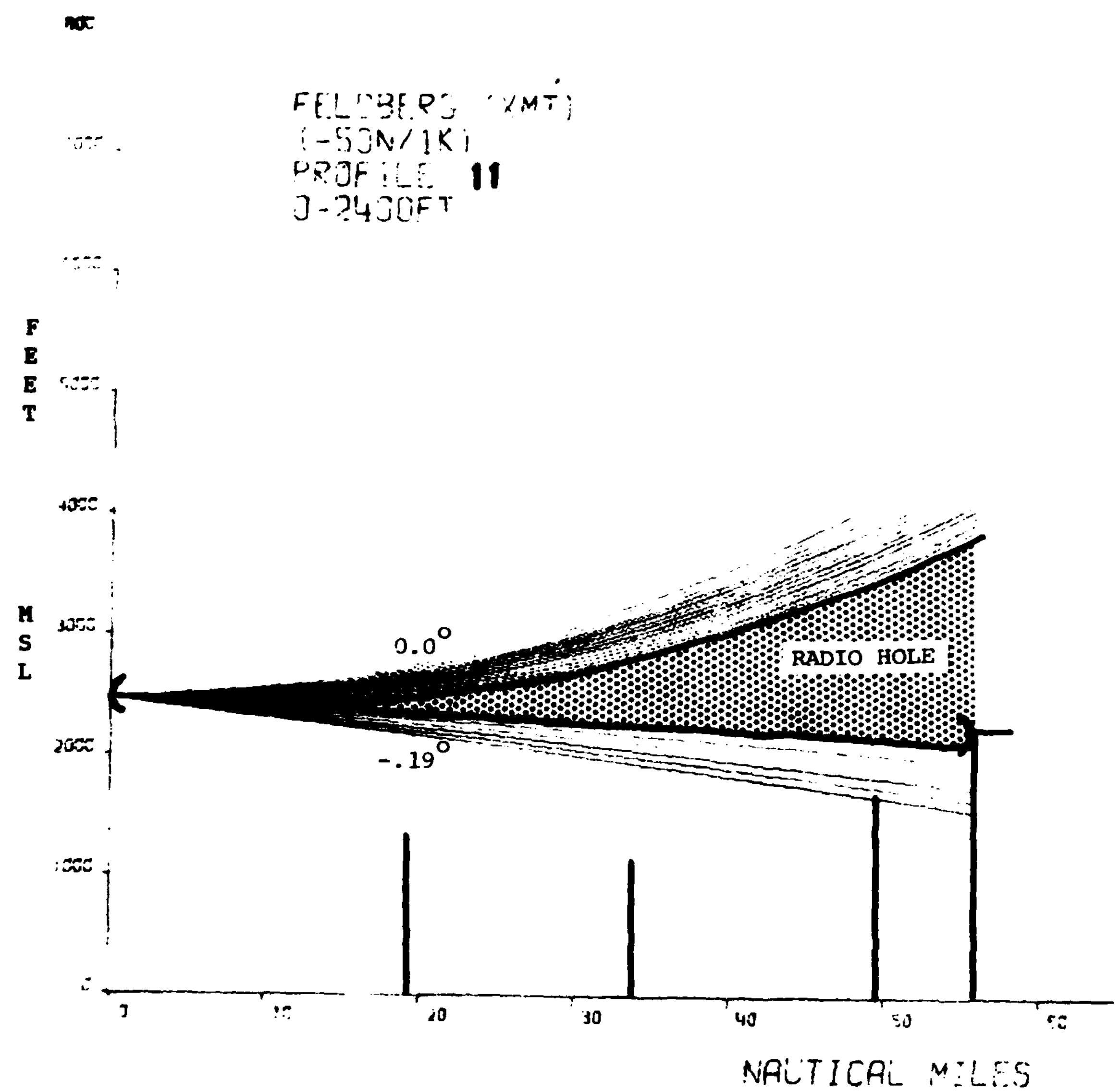

Figure 16. Detail of Ray Tracing for Profile #11

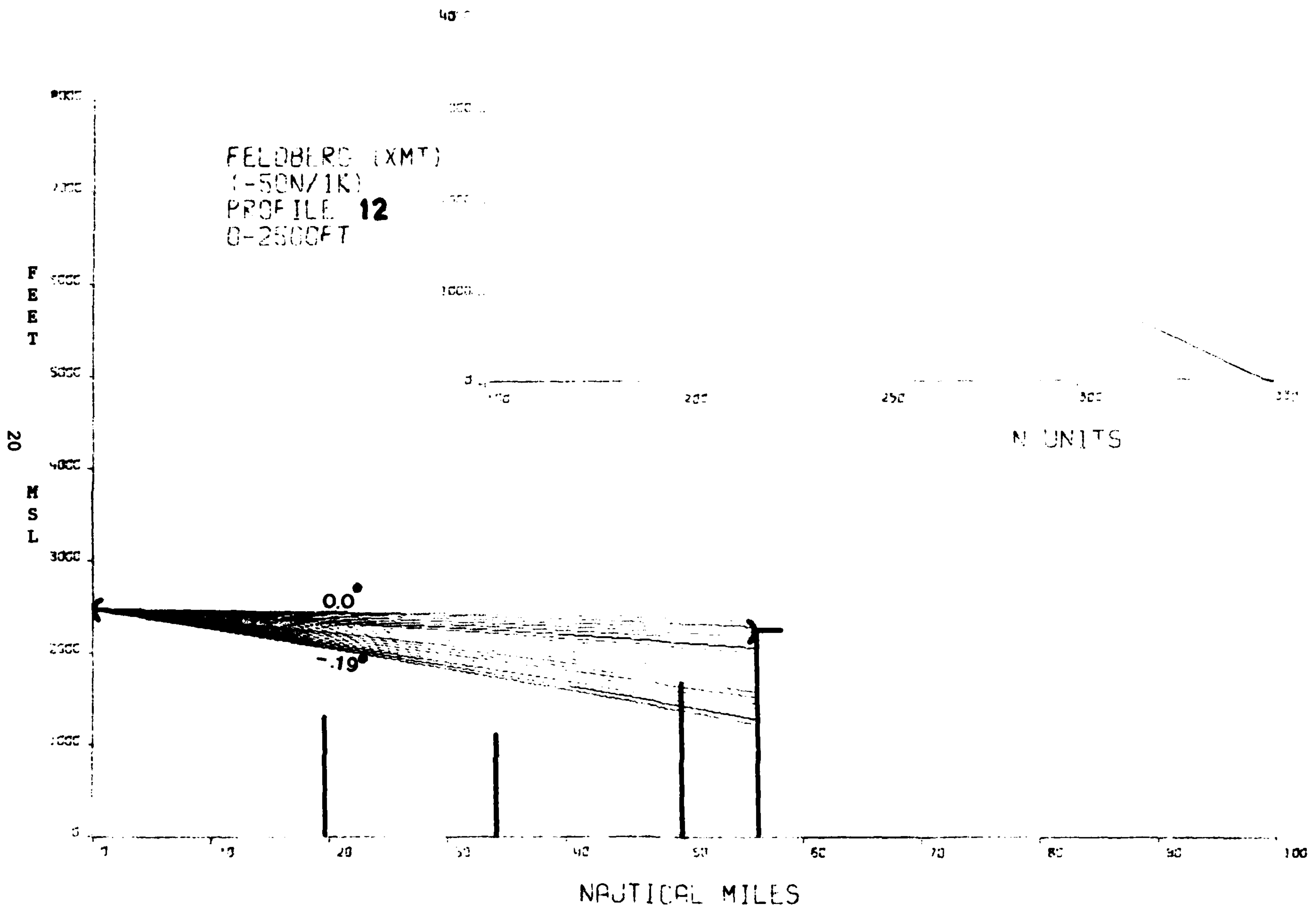

Figure 17. Refractivity Profile #12 and Ray Tracing for Layer 0-2500 ft MSL

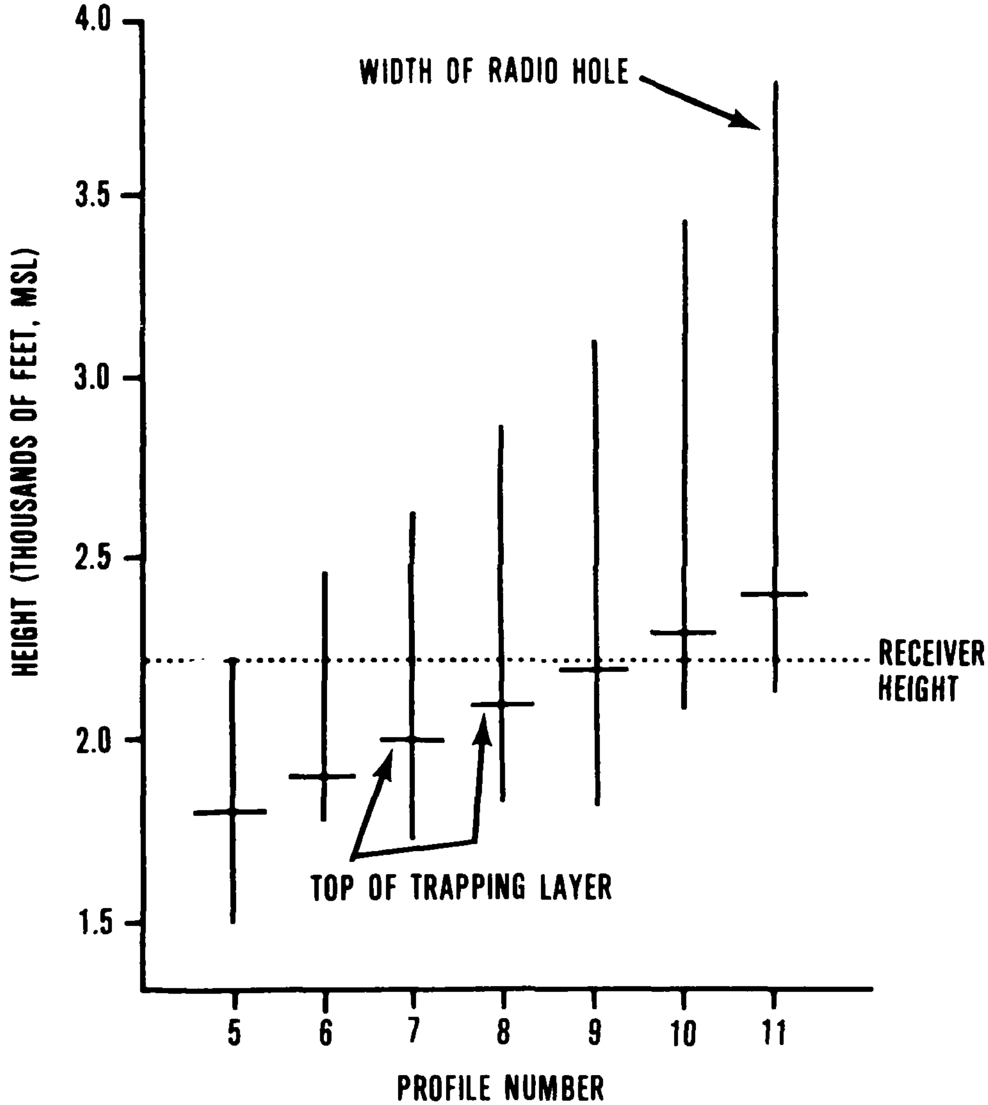

Figure 18. Width of Holes and Location Relative to Receiver

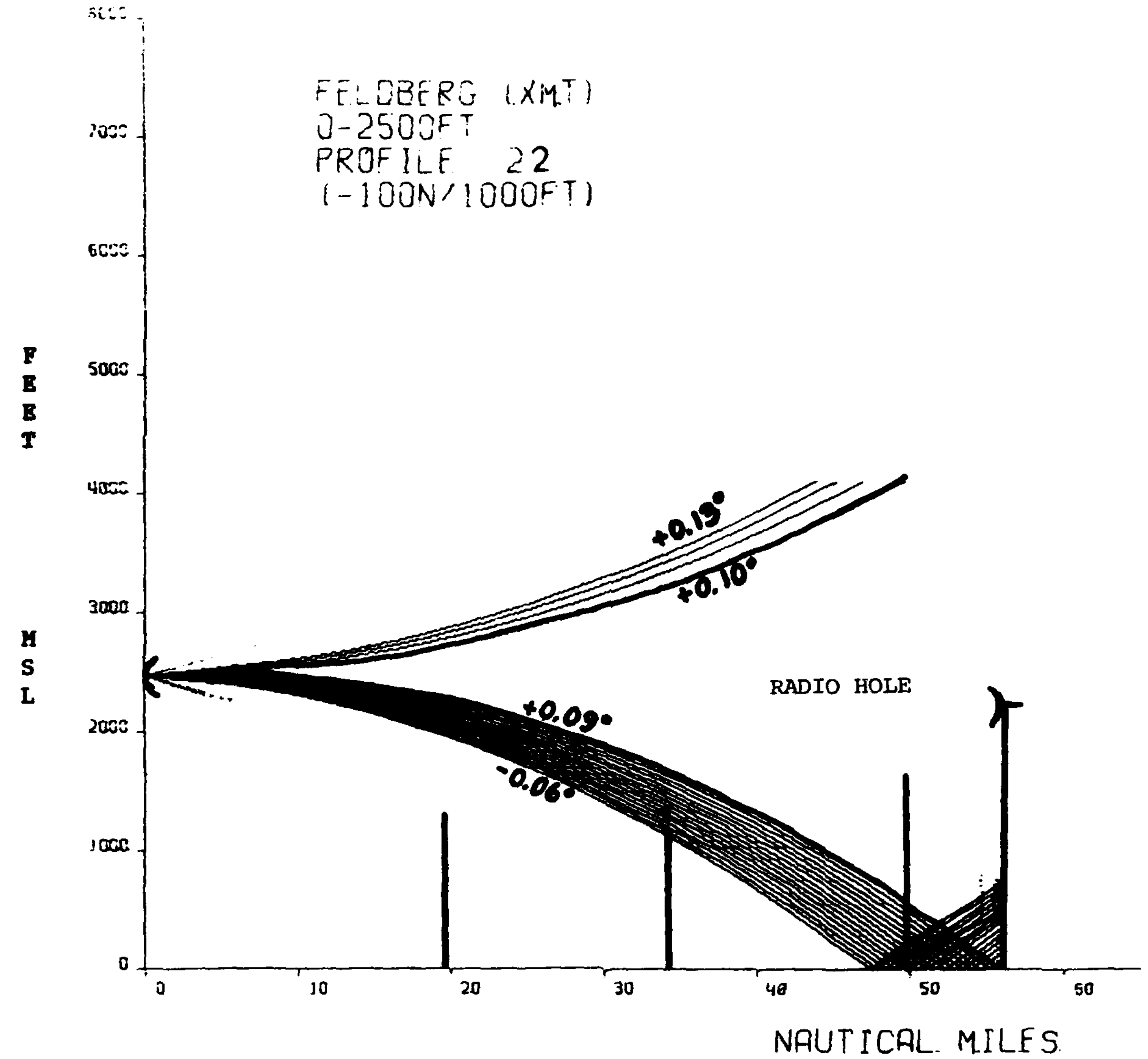

Figure 19. Ray Tracing for Layer 0-2500 ft MSL and Refractivity Gradient -100N/1000 ft

DISTRIBUTION LIST
7WW/TN-82/001

HQ MAC/HO	1
HQ AWS/DNT	1
2WS/DO	1
1WW/DN	1
30WS	1
2WW/DN	1
7WS	1
28WS	1
31WS	1
3WW/DN	1
9WS/DON	1
11WS/DN	1
12WS/DN	1
26WS/DN	1
5WW/DN	1
1WS	1
3WS	1
5WS	1
6WS	1
24WS	1
25WS	1
7WW/DO	25
15WS	1
17WS/DON	1
AFCC Liaison	20
3350/TCHTG/TTGW-W	1
AFGWC(DO, TS, WF)	3
USAFETAC(DAJ, DN, ENA, TS, TSK)	5
AWSTL	25
Total Printed	102

FILME

9